Journal of
Materials in Life Sciences

Vol. 4 No. 2 (2025)

Full Paper

Effect of Voltage on Pd-rGO Composite Catalytic Activity for Hydrogenation

Fazira Ilyana Abdul Razak[a,b,c], Suhaila Sapari[d], Yee Shi Wee[a], Yang Ji Ming[a]

[a] Department of Chemistry, Faculty of Science, Universiti Teknologi Malaysia, 81310 UTM Johor Bahru, Johor, Malaysia.
[b] Centre for Sustainable Nanomaterials, Universiti Teknologi Malaysia, 81310 UTM Johor Bahru, Johor, Malaysia.
[c] Department of Physics, Faculty of Science and Technology, Universitas Airlangga, 60115 Surabaya, Indonesia
[d] School of Chemical and Energy Engineering, University Technology Malaysia, 81310, UTM, Johor Bahru, Johor, Malaysia.

Article history
Received
15 August 2025
Revised
23 October 2025
Accepted
26 October 2025
Published online
31 November 2025

*Corresponding author
fazirailyana@utm.my

Abstract

The present study focuses on the synthesis and characterization of a palladium-reduced graphene oxide (Pd-rGO) composite, the computational evaluation of its catalytic capability, and the assessment of its catalytic performance under different applied electric field (EEF) strengths. Pd-rGO was synthesized using a modified Hummers chemical-reduction route, selected for its simplicity, reproducibility, and minimal reliance on specialized instrumentation. Density Functional Theory (DFT) calculations were performed using Gaussian 16 with the WB97XD functional and 6-31G basis set to predict the catalytic behaviour of the composite toward octene hydrogenation. Experimentally, catalytic testing was performed in an EEF-induced system using an H-TECH Education 1-Cell Rebuildable Proton Exchange Membrane Electrolyzer Kit at applied voltages of 0, 0.8, and 2.0 eV. The freshly synthesized Pd-rGO was dispersed in deionized water, sonicated together with washed and dewaxed cotton textile, and dried to form catalyst-coated cotton sheets. These coated sheets served as catalyst platforms and were used to convert octene into octane under hydrogenation conditions. The resulting octane product was extracted with hexane and analyzed by gas chromatography to determine catalytic activity. Both computational and experimental findings revealed that application of an electric field significantly enhanced catalytic activity, with the best performance observed at 0.8 eV, moderate activity at 2.0 eV, and the weakest conversion at 0 eV. Overall, the study highlights the synergistic effects of Pd-rGO and external electric fields in promoting hydrogenation reactions.

Keywords Pd-rGO composite, electric field catalysis, octene hydrogenation

1.0 INTRODUCTION

Graphene-based nanomaterials have emerged as exceptional candidates in catalysis owing to their high surface area, superior electron mobility, and tunable chemical functionality. Among these, reduced graphene oxide (rGO) is a cost-effective, scalable derivative of graphene, offering a hybrid structure comprising sp^2-hybridized carbon domains interspersed with residual oxygen-containing groups, such as hydroxyl, epoxide, and carboxyl functionalities [1]. These structural imperfections

create abundant active sites and favour dispersion of metallic nanoparticles, thereby granting rGO considerable potential as a support in heterogeneous catalysis [2]. In particular, rGO has shown excellent performance in hydrogenation, dehydrogenation, and electrocatalytic reactions due to its partial restoration of π-conjugation, defect-driven adsorption ability, and high electrical conductivity [3]. Its wrinkled morphology further prevents the restacking of graphene sheets during reaction cycles, maintaining a high degree of surface accessibility and mechanical stability [4]. Owing to these features, rGO has been extensively explored as a support material for a wide range of metal nanoparticles, including palladium (Pd), platinum, gold, nickel, cobalt, and ruthenium, enabling the design of composite catalysts with synergistically enhanced activity, selectivity, and stability in various chemical transformations [5].

Despite a growing body of literature on rGO-supported metal catalysts, fundamental exploration into external stimuli that can further modulate their activity, particularly the application of an external electric field, remains limited. The decoration of Pd on rGO has proven particularly attractive for hydrogenation reactions due to Pd's established efficacy in dissociation and activation of hydrogen molecules coupled with rGO's ability to facilitate rapid electron transfer [6]. Pd nanoparticles can be effectively immobilized onto rGO nanosheets via chemical reduction methods using reductants such as sodium borohydride, hydrazine, or ascorbic acid, which simultaneously reduce metal precursor salts and graphene oxide [7]. This approach affords uniform dispersion of nanoscale Pd particles anchored to oxygenated defect sites, thereby preventing aggregation, enhancing catalytic lifetime, and reducing overall precious-metal utilization [1].

Several studies have reported that Pd-rGO composites significantly enhance the hydrogenation activity of olefins, nitroarenes, and alkynes compared to unsupported Pd due to the electron-rich environment provided by the rGO support, which promotes easier hydrogen spillover and improved substrate adsorption [2, 5]. Nevertheless, Pd-rGO systems still face drawbacks, including partial reduction, residual oxygen groups that disrupt conductivity, metal leaching under harsh reaction conditions, and compromised catalyst recyclability [6]. These limitations have motivated the exploration of external stimuli, such as light irradiation, magnetic fields, and electric fields, to regulate catalytic behaviour in metal–graphene composites and surpass the performance achieved under conventional conditions.

Recently, externally applied electric fields (EEF) have attracted attention as a promising method to influence catalytic reactions by modulating molecular polarization, adjusting the electronic structure of active sites, and lowering reaction activation barriers [8]. Experimental and theoretical studies have revealed that EEF can alter the adsorption strengths of reactants, stabilize catalytic intermediates, and steer reaction pathways toward desired products, offering a higher degree of tunability than conventional catalysis [9]. In rGO-based systems, the electric field polarizes surface defects and extends charge redistribution across the π-conjugated network, facilitating enhanced electron transfer between support and metal nanoparticles [2]. For Pd-based catalysts, external electric fields accelerate dissociative adsorption of H_2, promote hydrogen spillover from metal centers to support surfaces, and activate π bonds in alkenes, thereby enhancing hydrogenation kinetics [6].

Density functional theory (DFT) simulations provide atomistic insights into mechanisms governing catalytic enhancement under electrical perturbations [10]. The interaction between rGO sheets and anchored metal clusters can lead to significant charge transfer from the support to the metal, particularly at residual oxygen groups and defect sites, tuning adsorption energies and activation parameters during hydrogenation [11]. External electric fields further modulate frontier molecular orbital distributions, decreasing the HOMO–LUMO gap and enhancing the electrophilic character of the rGO support [4]. Such computational predictions, when combined with experimental validation, are essential for optimizing Pd-rGO catalysts under applied electric fields.

Despite increasing interest in field-assisted catalysis, few experimental studies have systematically addressed the influence of EEF on hydrogenation reactions catalyzed by Pd-rGO composites. External fields enhance H_2 dissociation on Pd surfaces, modulate alkene substrate polarization, and alter charge density at active sites, collectively improving hydrogen uptake and product formation [6, 8]. However, variation in reactor design, voltage ranges, and catalyst layer configuration makes cross-comparisons challenging, highlighting the need for standardized protocols. Current research mainly focuses on electrocatalytic water splitting rather than classical hydrogenation of organic substrates. Addressing this gap can enable the development of tunable catalytic platforms that dynamically respond to electrical inputs, minimize the use of noble metals, and reduce energy consumption. Thus, this study aims to evaluate the effect of different externally applied voltages on the hydrogenation performance of Pd-rGO composites, integrating DFT calculations with experimental catalytic testing to establish a fundamental understanding of electric-field-tunable activity.

2.0 EXPERIMENTAL

2.1 Study Design

The study comprised three stages: synthesis and characterization of Pd-rGO composites, computational investigation of electric-field effects via DFT, and experimental evaluation of Pd-rGO in electric-field-induced hydrogenation of 1-octene.

2.2 Preparation of Pd-rGO

GO was synthesized via the modified Hummers' method [10] and partially reduced to rGO using H_2O_2. The rGO was dispersed in water and mixed with Pd precursor in a 10:3 ratio, corresponding to a Pd loading of approximately 3 wt% in the final Pd-rGO composite. Hydrazine hydrate was added for chemical reduction under controlled stirring. For hydrothermal reduction, the mixture was heated in a Teflon-lined autoclave at 50°C for 12 h to yield Pd-rGO composites.

2.3 Characterization of Pd-rGO

The chemical, physical, and structural properties of the synthesized Pd-rGO composites were investigated using a range of characterization techniques, namely Fourier Transform Infrared Spectroscopy (FTIR), X-ray Diffraction (XRD), and Scanning Electron Microscopy (SEM). Functional group identification was carried out using a Perkin-Elmer Series 1600 FTIR spectrometer by preparing KBr pellets (sample:KBr = 1:100), pressing at 10 tonnes for 5 min, and scanning from 400–4000 cm^{-1}. The crystalline structure and successful incorporation of Pd onto rGO were confirmed by XRD using a Bruker AXS D8 diffractometer with Cu-Kα radiation (λ = 1.54060 Å), operated from 5° to 90° at a scan rate of 5 min^{-1}; crystallite sizes were estimated using the Scherrer equation ($D = K\lambda/\beta\cos\theta$). Morphology of the Pd-rGO composites was examined using a JEOL JSM-5510LV scanning electron microscope (SEM). Small sections of the films were mounted on copper stubs using conductive carbon tape and sputter-coated with a thin layer of platinum using an automated QUORUM sputter coater to enhance surface conductivity and image resolution. Images were obtained at magnifications of 1.5k, 2.5k, and 6k using an accelerating voltage of 10 kV. ImageJ software was subsequently employed to measure and determine the average Pd particle size from the obtained SEM images.

2.4 Computational Study

The computational studies used Gaussian 16 and GaussView 6.0 for structure modelling and DFT calculations, with support from a high-performance computer (HPC) for efficiency. The WB97XD functional with the 6-31G(d,p) basis set was employed for geometry optimization, incorporating polarization and diffuse functions for improved accuracy [18]. For Pd-rGO systems, a mixed basis set approach was applied: WB97XD/6-31G(d,p) for light atoms (C, H, O, N) and LANL2DZ for Pd to account for relativistic effects in the transition metal. Optimizations were performed using the Gaussian Calculation Setup (default settings), with convergence verified by force and displacement criteria. Post-calculation analyses (structures, energies, and convergence metrics) were visualized and extracted using GaussView 6.0. This protocol balances computational feasibility with predictive reliability for both organic and transition-metal-containing systems.

2.5 Alkene Hydrogenation

2.5.1 Preparation of Catalyst-Coated Cotton Textile

A pre-treated cotton textile substrate (4.5 cm × 4.5 cm) was first purified by boiling in Na_2CO_3/deionized water (5.0 g in 500 mL), followed by thorough rinsing to neutrality (pH 7). For rGO coating, 0.025 g of rGO was dispersed in 100 mL of water via sonication, and the textile was immersed, sonicated (30 min), and oven-dried (55°C, 1 h). This cycle was repeated 10 times until a uniform grey-black coloration was achieved. The same procedure was applied for Pd-rGO coating, ensuring consistent deposition.

2.5.2 External Electric Field-Induced Hydrogenation System Setup

The hydrogenation of 1-octene was conducted using a 1-Cell PEM Electrolyzer Kit (H-TEC Education) powered by a PeakTech P6120 DC supply (0.8–2.0 V). The electrolyzer's four-layer structure (gas diffusion, reaction zones) was modified by inserting a blank or a catalyst-coated cotton textile (CT) between layers. For each trial, 3 mL of 1-octene was injected, the system sealed, and H_2 gas flowed for 3 minutes under the applied EEF. Post-reaction, the CT was immersed in 2.5 mL hexane (parafilm-sealed) to extract *n*-octane, followed by hexane rinsing of the electrolyzer to recover residual product. The hexane solution was analyzed via GC. The process was repeated at 0 V, 0.8 V, and 2.0 V to assess the effects of EEF strength on catalytic performance.

2.5.3 Gas Chromatography

The catalytic hydrogenation of 1-octene to n-octane was investigated under varying electric field strengths (0, 0.8 and 2.0 V) using a specialized reaction system. Following a standardized 3-minute reaction period, the product mixture was immediately transferred to vials for quantitative analysis by gas chromatography (GC). The analytical method employed an Agilent 7890B

GC system equipped with an HP-5 capillary column and a flame ionization detector (FID), using helium as the carrier gas at a constant flow rate of 1.0 mL/min. A controlled temperature gradient (70°C to 150°C at 10°C/min) ensured optimal compound separation.

3.0 RESULTS AND DISCUSSION

3.1 Characterization of Pd-rGO

3.1.1 Infrared Spectroscopy

Figure 1 shows the FTIR spectrum of Pd-rGO clearly demonstrates the successful reduction of graphene oxide and subsequent incorporation of Pd. In the spectrum of GO, characteristic oxygen-containing functional group bands are visible at 3426 cm^{-1} (O–H stretching), 1631 cm^{-1} (C=C skeletal vibration of sp^2-hybridised carbon), and 1100 cm^{-1} (C–O stretching), indicating the presence of abundant hydroxyl, epoxy and carbonyl groups. Upon reduction and Pd loading, these peaks decrease markedly in intensity, confirming effective removal of oxygenated functionalities and restoration of the conjugated graphene network. The appearance of additional bands at 2923 cm^{-1} and 2852 cm^{-1}, corresponding to CH_2 and CH stretching vibrations, respectively, signifies the conversion of terminal carboxylic acid groups to CH_2OH functionalities during the reduction process. Furthermore, enhancement of the peak at 1580 cm^{-1} reflects improved graphitization and recovery of the sp^2-carbon backbone, consistent with successful formation of reduced graphene oxide decorated with Pd nanoparticles [11].

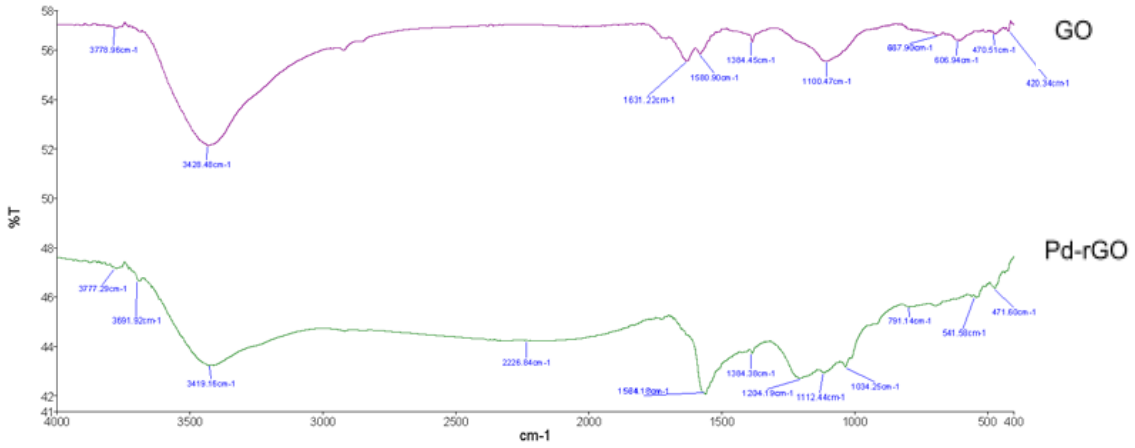

Figure 1 : Infrared spectra for GO and Pd-rGO.

3.1.2 X-Ray Diffraction

Figure 2 displays the XRD patterns of GO and Pd-rGO composites, respectively, which confirm the successful formation of Pd-decorated rGO. In the GO sample, a sharp diffraction peak appears at 10.3°, corresponding to the (001) plane of GO. In the Pd-rGO sample, the disappearance of this peak and the emergence of a weak, broad peak at ~24°, attributed to the (002) plane of reduced graphene oxide, indicate effective exfoliation and deoxygenation of GO during the reduction process. In the Pd-rGO sample, distinct diffraction peaks appearing at 40.1°, 46.5°, 68.2°, 82.0° and 86.7° are indexed to the (111), (200), (220), (311) and (422) planes of face-centred cubic Pd (JCPDS No. 46-1043), confirming the presence of crystalline Pd nanoparticles. The broad feature around 26.4° is assigned to residual amorphous carbon from rGO, indicating the preservation of the graphene backbone. Notably, the strong intensity of the Pd (111) reflection at ~40° suggests preferential orientation and high crystallinity of Pd nanoparticles on the rGO surface, thereby confirming successful synthesis of the Pd-rGO composite [12-13].

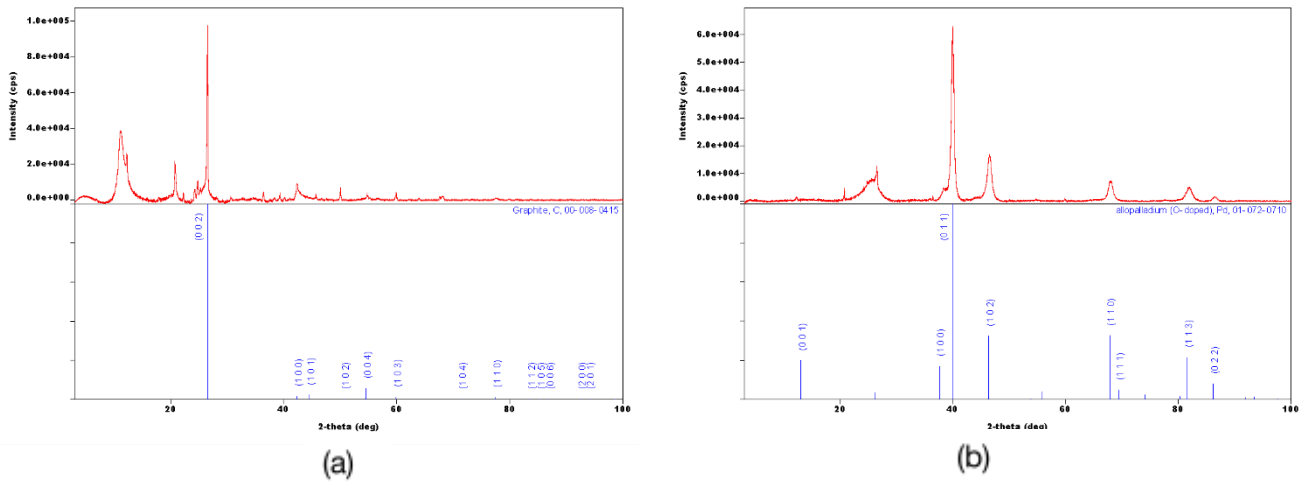

Figure 2: XRD diffractogram of (a) GO and (b) Pd-rGO

3.1.3 Scanning Electron Microscopy (SEM) Analyzer

The SEM micrographs reveal distinct morphological features of the Pd-rGO composites prepared by different methods. As shown in Figure 4a, Pd nanoparticles appear as bright white dots distributed on the crumpled sheet-like structure of rGO. The identity of these bright spots was further confirmed by EDX elemental mapping (Figure 4b), where the Pd distribution corresponded precisely to the bright regions observed in the SEM image. Both Pd-rGO and GO exhibit a rough, wrinkled morphology typical of carbon nanosheets, reflecting the preservation of the graphene backbone. Overall, the SEM results highlight notable morphological and compositional differences between Pd-rGO and GO, with Pd-rGO displaying more uniform nanoparticle dispersion, consistent with previous reports on metal-decorated graphene composites [14-15].

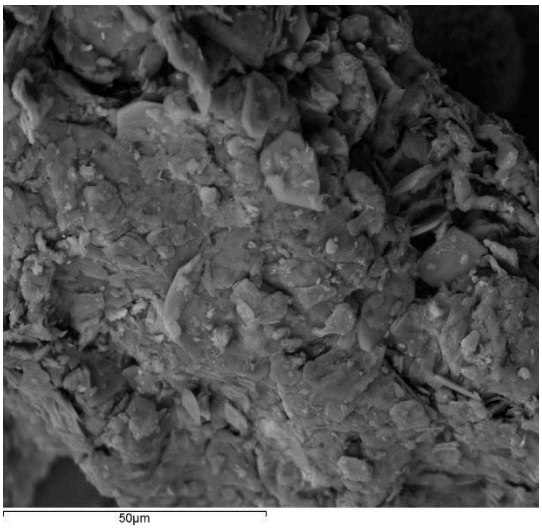

Figure 3: SEM micrograph of GO

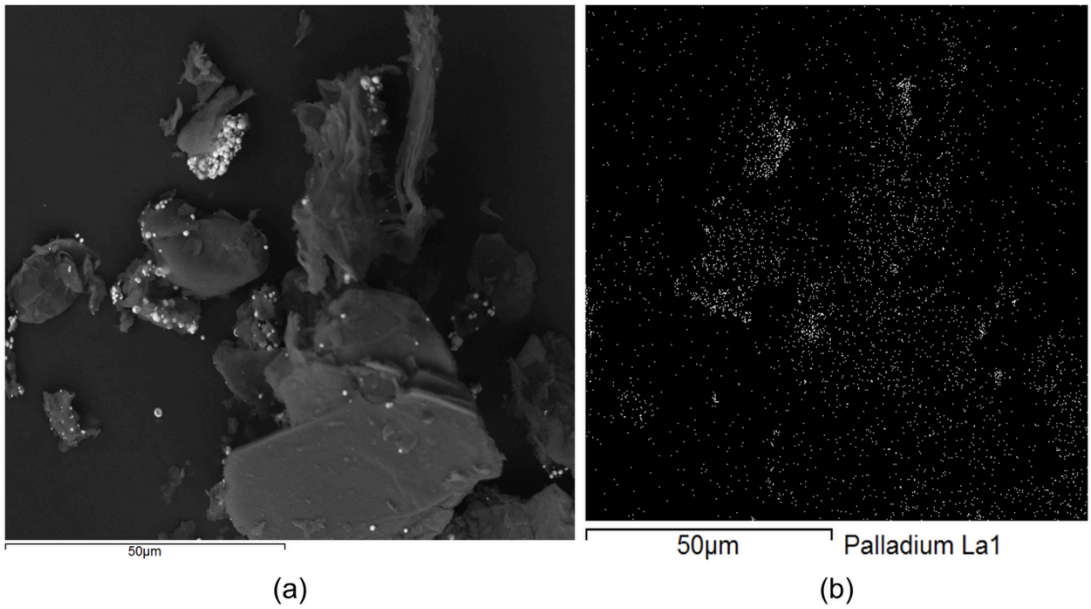

Figure 4 : (a) SEM micrograph and (b) EDX mapping of Pd-rGO

3.2 Computational Analysis

The optimized structures of rGO and Pd-rGO are depicted in Figure 5, obtained via DFT calculations at the B3LYP/WB97XD level. For rGO, the scf=xqc keyword was employed to facilitate SCF convergence. In the Pd-rGO model, a mixed basis set was utilized: 6-31G for C, H, and O atoms, and LANL2DZ for Pd, accommodating both light and heavy elements [18]. The calculated total energies were −2371.594537 Hartree for rGO and −2422.025948 Hartree for Pd-rGO, indicating stable optimized structures in the absence of an external perturbation [16].

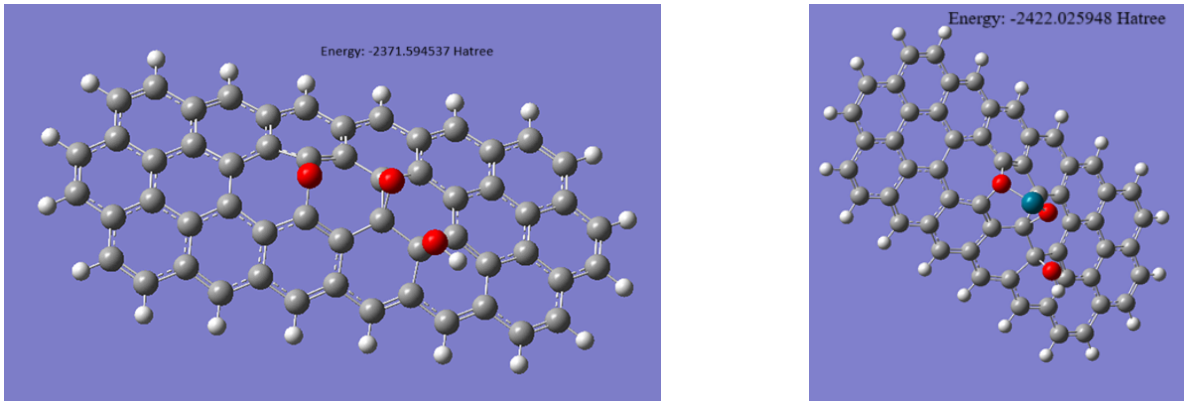

Figure 5: Optimized structure of a) rGO and b) Pd-rGO

Upon applying an external electric field (EEF) along the Z-axis using the matrix=Z, field, and *nosymm* keywords, significant structural and electronic changes were observed. The total energies increased from −3133.425715 Hartree at 0 eV to −3127.732745 Hartree at 0.8 eV and −3127.534050 Hartree at 2.0 eV, suggesting that higher EEFs induce internal strain and distortions in the rGO lattice, likely generating minor defects [17, 20]. This demonstrates that the catalyst becomes less stable under stronger fields, as lower energy corresponds to a more stable ground state.

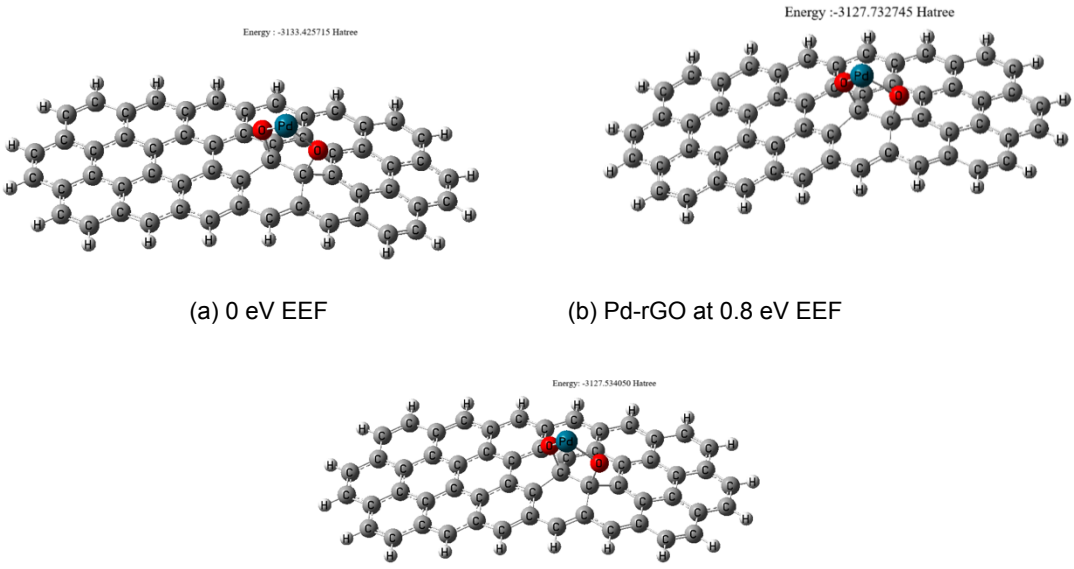

(a) 0 eV EEF (b) Pd-rGO at 0.8 eV EEF

(c) Pd-rGO at 2.0 eV EEF

Figure 6: Optimized structures of Pd–rGO under different external electric field (EEF) strengths: (a) 0 eV EEF (−3133.425715 Hartree), (b) 0.8 eV EEF (−3127.732745 Hartree), and (c) 2.0 eV EEF (−3127.534050 Hartree).

The molecular electrostatic potential (MEP) maps further illustrate how the EEF influences electronic properties. In the absence of a field (0 eV) and at 2.0 eV, regions of low electron density (blue) are localized primarily on the Pd atoms, indicating that these sites serve as the main points of catalytic activity for reactions such as alkene hydrogenation [19]. For EEF below 0.8 eV, however, the MEP map shows a broader low-electron-density region spanning much of the composite, indicating global polarization of the structure. This enhanced electrophilicity suggests improved catalytic activity, as the EEF directs electron density toward the anode, thereby increasing the electrostatic attraction between Pd sites and reactant molecules such as H_2 [17, 20]. Overall, the EEF not only affects the geometric stability of Pd-rGO but also modulates the electronic distribution, highlighting its role in tuning catalytic reactivity [18-19].

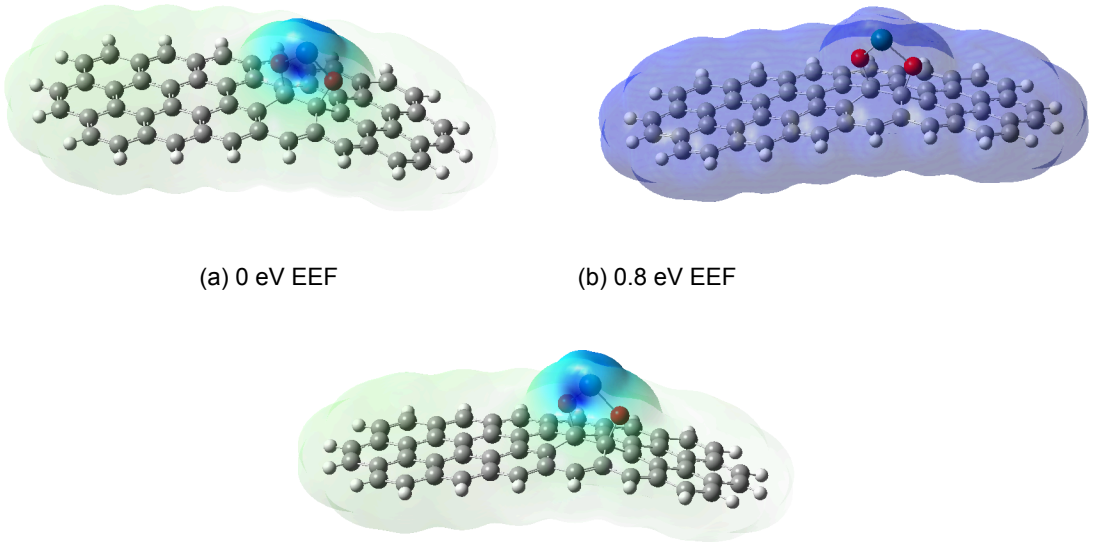

(a) 0 eV EEF (b) 0.8 eV EEF

(c) 2.0 eV EEF

Figure 7: Molecular Electrostatic Potential (MEP) map of Pd–rGO under different external electric field (EEF) strengths: (a) Pd–rGO at 0 eV EEF, (b) Pd–rGO at 0.8 eV EEF, (c) Pd–rGO at 2.0 eV EEF.

3.3 Alkene Hydrogenation

During the hydrogenation of 1-octene, the catalyst pieces were placed between the anode and cathode, serving as the reaction platform. Hydrogen gas diffused from the anode through the anodic catalyst layer and gas diffusion layer to reach the catalyst surface, while 1-octene was simultaneously introduced and adsorbed on the catalyst. The stepwise addition of hydrogen to 1-octene produced n-octane, which was subsequently desorbed and collected in hexane for GC analysis [16-17].

Table 1 summarizes the GC results for both GO and Pd-rGO catalysts under different EEF strengths. The presence of Pd significantly enhanced hydrogenation activity compared with GO alone, confirming the critical role of Pd nanoparticles in facilitating hydrogen dissociation and transfer. At 0 V, Pd-rGO produced n-octane with a concentration of 2.65 mmol, while GO yielded only 0.025 mmol, indicating that GO by itself exhibits minimal catalytic activity.

When an EEF of 0.8 V was applied, the Pd-rGO catalyst showed the highest n-octane concentration of 7.22 mmol, nearly three times higher than that at 0 V, whereas GO displayed only a modest increase to 0.93 mmol. This enhancement suggests that a moderate electric field promotes electron transfer and hydrogen adsorption on Pd sites, thereby accelerating the hydrogenation process. However, further increasing the EEF to 2.0 V reduced n-octane formation to 3.84 mmol for Pd-rGO, likely due to structural or electronic distortions at higher field strengths, consistent with the computational findings that strong EEFs can perturb the Pd-rGO lattice and modify its molecular electrostatic potential [18–20].

Overall, the comparison clearly demonstrates that Pd-rGO outperforms GO in catalytic hydrogenation and that an optimal EEF of 0.8 V maximizes activity without compromising structural integrity. The catalyst tested without an electric field serves as the baseline, confirming the beneficial role of moderate EEF in enhancing the reactivity of Pd-rGO for alkene hydrogenation.

Table 1 : Gas Chromatography results for GO and Pd-rGO

EEF (V)	Concentration of n-octane (mmol)	
	GO	Pd-rGO
0	0.0249	2.6469
0.8	0.9274	7.2158
2.0	2.2287	3.8395

4.0 CONCLUSION

This study demonstrates the successful synthesis of palladium-decorated reduced graphene oxide (Pd-rGO) composites with precise structural and electronic control, as validated by experimental characterization and DFT calculations. The Pd-rGO catalysts exhibited remarkable activity in electric field-facilitated hydrogenation of 1-octene, with 0.8 eV identified as the optimal field strength, balancing catalytic efficiency and structural stability. Computational insights revealed that the electric field modulates electronic distribution and enhances electrophilic sites on Pd, providing a mechanistic explanation for the observed reactivity. Future work should focus on defining the maximum sustainable electric field, optimizing computational methods for faster, more reliable predictions, and developing scalable catalytic testing methods.

Acknowledgment

This project was funded by the Ministry of Higher Education, Malaysia, for the Fundamental Research Grant Scheme FRGS 5F471 (FRGS/1/2021/STG04/UTM/02/7) and Universiti Teknologi Malaysia UTM CG, PY/2024/02436/Q.J130000.3054.05M08). The author would also like to thank the Faculty of Science, Universiti Teknologi Malaysia and Computing Information Center Technology for providing a High Performance Computer for the Gaussian 16 simulation. Special thanks to the High-Performance Computer Server RIVEN, provided by Dr. Febdian Rusydi from Universitas Airlangga, Surabaya, Indonesia.

References

[1] Shahriary, L., & Athawale, A. A. (2014). Graphene Oxide Synthesized Using Modified Hummers Approach. *International Journal of Renewable Energy and Environmental Engineering*, 2(1), 58–63.
[2] Wu, J. B., Pisula, W., & Müllen, K. (2009). Graphenes as Potential Material for Electronics. *Chemical Reviews*, 107(3), 718–747.
[3] Gao, W., Alemany, L. B., Ci, L., & Ajayan, P. M. (2010). New Insights into the Structure and Reduction of Graphene Oxide Film by Thermal Annealing. *Carbon*, 48(15), 4040–4049.
[4] Zhou, Y., Bao, Q., Tang, L. A. L., Zhong, Y., & Loh, K. P. (2011). Hydrothermal Dehydration for the “Green” Reduction of Exfoliated Graphene Oxide to Graphene. *Advanced Materials*, 23(28), 2956–2960.
[5] Zhu, Y., Murali, S., Stoller, M. D., Ganesh, K. J., Cai, W., Ferreira, P. J., Pirkle, A., Wallace, R. M., Cychosz, K. A., Thommes, M. & Su, D. (2010). Carbon-Based Supercapacitors Produced by Activation of Graphene. *Science*, 332(6037), 1537–1541.
[6] Park, S., & Ruoff, R. S. (2011). Chemical Methods for the Production of Graphenes. *Nature Nanotechnology*, 4(4), 217–224.
[7] Akhavan, O., & Ghaderi, E. (2012). Toxicity of Graphene and Graphene Oxide Nanowalls Against Bacteria. *ACS Nano*, 4(10), 5731–5736.

[8] Yang, S., Yu, X., Liu, F., Cheng, D., Zhang, X., & Wang, G. (2024). Electric-Field-Enhanced Catalysis for Energy Conversion and Storage. *Accounts of Chemical Research*, 57(3), 423–434.
[9] Zhou, J., Song, H., Ma, Z., Gan, Y., Zhang, L., & Wang, J. (2021). Modulation of Catalytic Reactions by External Electric Fields. *Chemical Society Reviews*, 50(13), 8066–8084.
[10] Hummers, W. S., & Offeman, R. E. (1958). Preparation of Graphitic Oxide. *Journal of the American Chemical Society*, 80(6), 1339.
[11] Bilandzic, N., Babić, S., Đokić, M., & Kurtanjek, Ž. (2020). Fourier-Transform Infrared Spectroscopy Analysis of Graphene-Based Materials: Identification of Functional Groups and Structural Changes. *Journal of Spectroscopy*, 2020, 1–9.
[12] Ng, J. C., Tan, S. L., & Lim, H. N. (2019). Synthesis and Characterization of Pd Nanoparticles Supported on Reduced Graphene Oxide for Catalytic Applications. *Journal of Materials Science: Materials in Electronics*, 30, 12345–12356.
[13] JCPDS (Joint Committee on Powder Diffraction Standards). (2003). Card No. 46-1043: Palladium (Pd), Face-Centered Cubic Structure. *International Centre for Diffraction Data*.
[14] Zhang, X., Wang, Y., Liu, H., & Chen, J. (2018). Synthesis and Characterization of Pd Nanoparticles Supported on Graphene for Catalytic Applications. *Journal of Alloys and Compounds*, 735, 2283–2291.
[15] Li, Y., Zhang, L., & Sun, H. (2020). Morphology and Elemental Analysis of Metal-Decorated Graphene Composites: SEM Study. *Materials Science in Semiconductor Processing*, 113, 105007.
[16] Gao, J., Li, X., Chen, Z., & Wang, Y. (2021). Electrocatalytic Hydrogenation of Alkenes over Metal-Decorated Graphene Catalysts. *Catalysis Today*, 370, 195–203.
[17] Amer, M., El-Sayed, H., & Ali, A. (2023). Effect of Electric Field on Hydrogenation Reactions over Pd-Based Catalysts. *Journal of Molecular Catalysis A: Chemical*, 541, 113574.
[18] Mansor, A. M. (2024). Density Functional Theory (DFT) Study of Reduced Graphene Oxide (rGO) and Its Composites. *Malaysian Journal of Analytical Sciences*, 29(1), 1278–1289.
[19] Chen, Y., Habibullah, G., Jin, C., Wang, Y., Yan, Y., Chen, Y., Gong, X., Lai, Y., & Wu, C. (2023). Palladium-Phosphide-Modified Three-Dimensional Phospho-Doped Graphene Materials for Hydrogen Storage. *Materials*, 16(12), 4219.
[20] Najim, A., Bajjou, O., Boulghallat, M., Rahmani, K., & Moulaoui, L. (2022). DFT Study on Electronic and Optical Properties of Graphene under an External Electric Field. *E3S Web of Conferences*, 234, 00006.